Supporting Information

```
        10          20          30          40          50          60
MEVCNCIEPQ WPADELLMKY QYISDFFIAI AYFSIPLELI YFVKKSAVFP YRWVLVQFGA

        70          80          90         100         110         120
FIVLCGATHL INLWTFTTHS RTVALVMTTA KVLTAVVSCA TALMLVHIIP DLLSVKTREL

       130         140         150         160         170         180
FLKNKAAELD REMGLIRTQE ETGRHVRMLT HEIRSTLDRH TILKTTLVEL GRTLALEECA

       190         200         210         220         230         240
LWMPTRTGLE LQLSYTLRHQ HPVEYTVPIQ LPVINQVFGT SRAVKISPNS PVARLRPVSG

       250         260         270         280         290         300
KYMLGEVVAV RVPLLHLSNF QINDWPELST KRYALMVLML PSDSARQWHV HELELVEVVA

       310         320         330         340         350         360
DQVAVALSHA AILEESMRAR DLLMEQNVAL DLARREAETA IRARNDFLAV MNHEMRTPMH

       370         380         390         400         410         420
AIIALSSLLQ ETELTPEQRL MVETILKSSN LLATLMNDVL DLSRLEDGSL QLELGTFNLH

       430         440         450         460         470         480
TLFREVLNLI KPIAVVKKLP ITLNLAPDLP EFVVGDEKRL MQIILNIVGN AVKFSKQGSI

       490         500         510         520         530         540
SVTALVTKSD TRAADFFVVP TGSHFYLRVK VKDSGAGINP QDIPKIFTKF AQTQSLATRS

       550         560         570         580         590         600
SGGSGLGLAI SKRFVNLMEG NIWIESDGLG KGCTAIFDVK LGISERSNES KQSGIPKVPA

       610         620         630         640         650         660
IPRHSNFTGL KVLVMDENGV SRMVTKGLLV HLGCEVTTVS SNEECLRVVS HEHKVVFMDV

       670         680         690         700         710         720
CMPGVENYQI ALRIHEKFTK QRHQRPLLVA LSGNTDKSTK EKCMSFGLDG VLLKPVSLDN

       730
IRDVLSDLLE PRVLYEGM
```

Fig. S1: Amino acid sequence of ETR1 from Arabidopsis thaliana (UniProt P49333). Glycine residues are indicated in red.

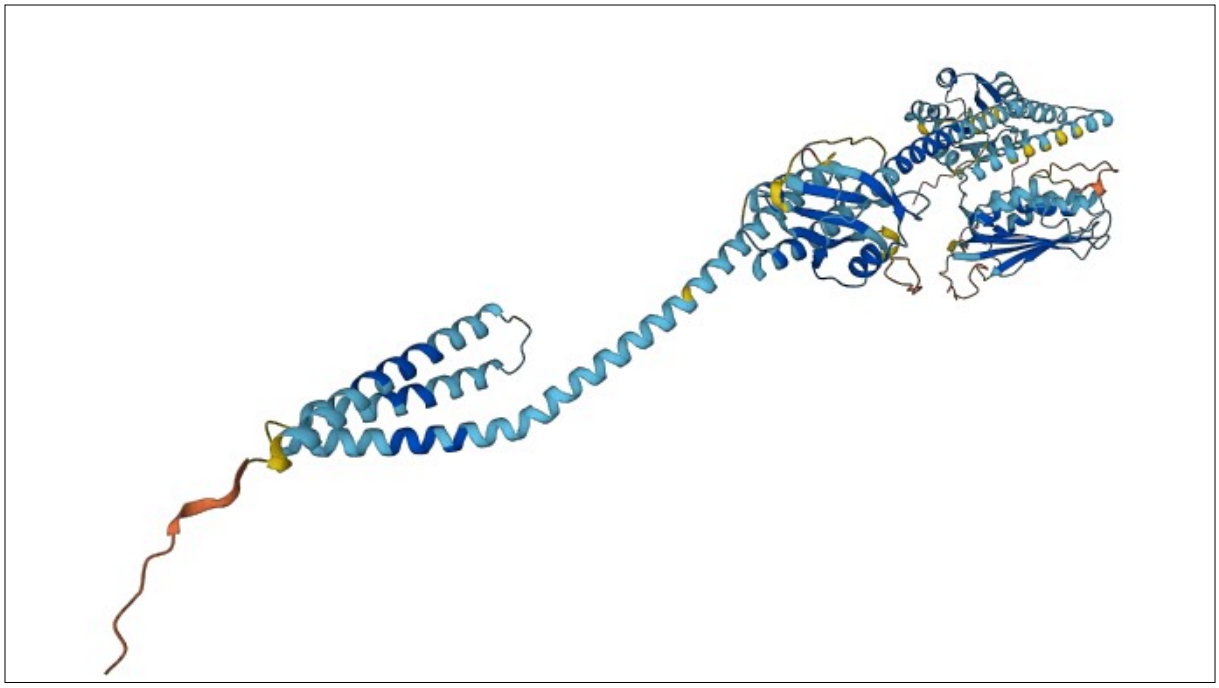

Fig. S2: AlphaFold 2.0. structural prediction of ETR1 from Arabidopsis thaliana (Uniprot P49333).

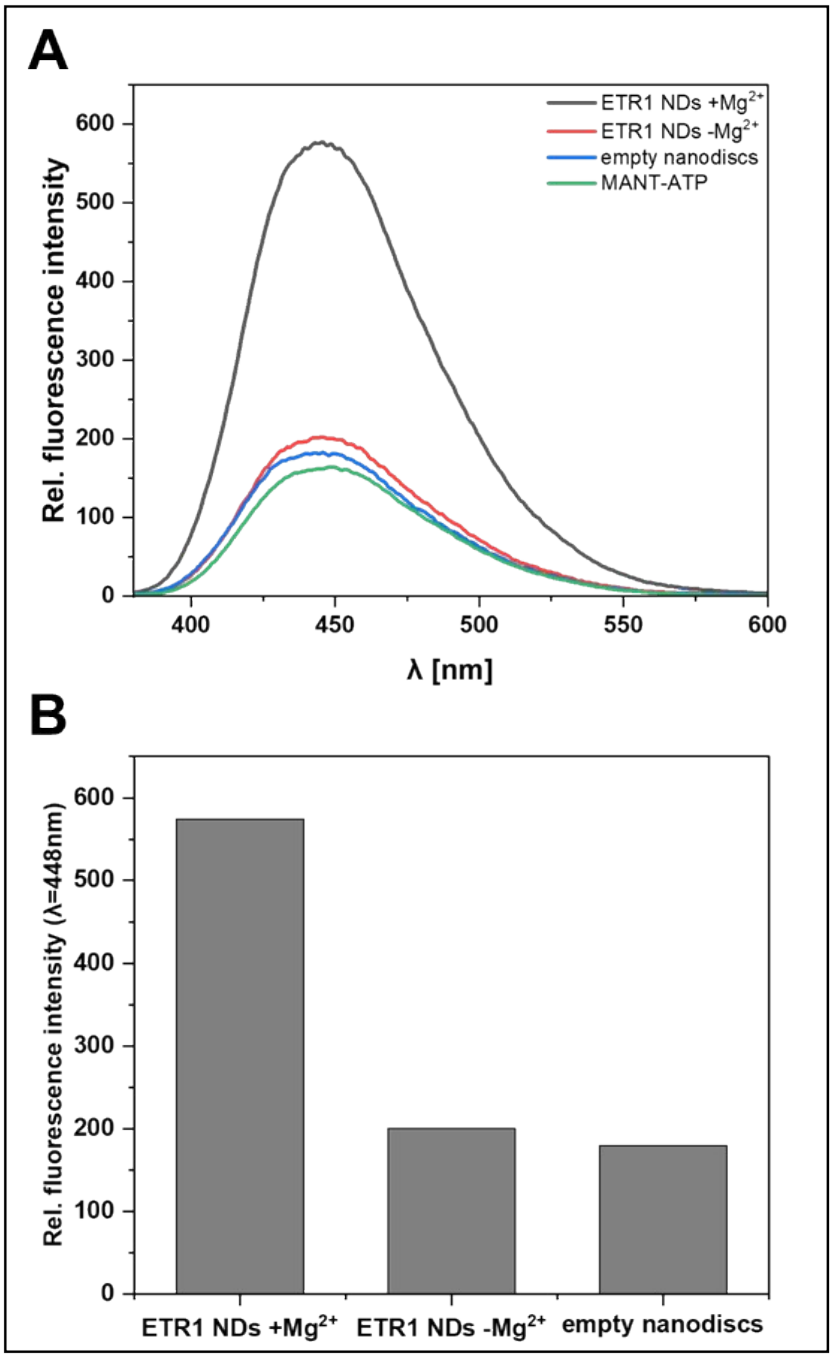

Fig. S3: Nucleotide Binding Assay. **A** Spectras of fluorescence intensities at wavelengths from 380nm until 600nm of ETR1 nanodiscs in presence of Mg^{2+} (black line) and in absence of Mg^{2+} (red line), empty nanodiscs (blue line) and MANT-ATP (green line). **B** Bar charts of relative fluorescence intensities measured at 448nm.

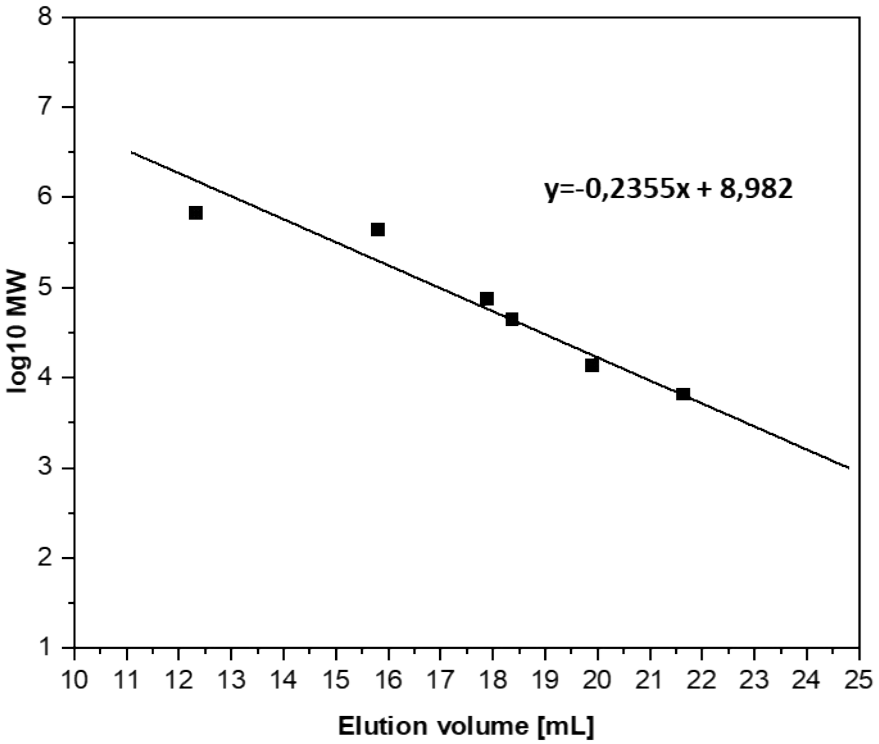

Calibration protein	MW [Da]	log10 MW	Elution volume [mL]
Dextran blue (V0)	2.000.000		9,15
Thyroglobulin	660.000	5,825	12,34
Ferritin	440.000	5,643	15,81
Conalbumin	75.000	4,875	17,9
Ovalbumin	44.000	4,643	18,37
Ribonuklease A	13.700	4,137	19,9
Aprotinin	6.500	3,813	21,65

Fig. S4: Calibration curve of size exclusion chromatography for Superose™ 6 Increase 10/300 GL column and table of used protein standards.

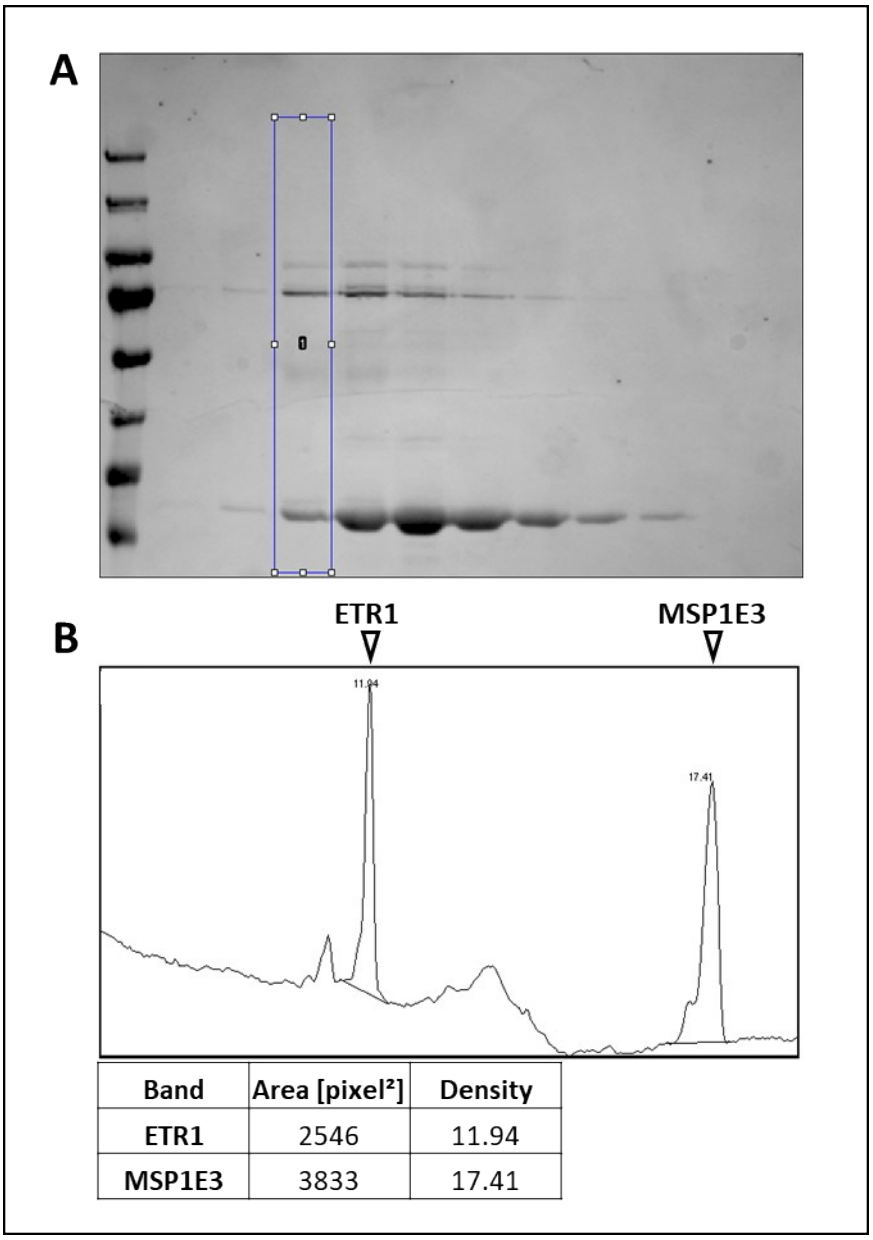

Band	Area [pixel²]	Density
ETR1	2546	11.94
MSP1E3	3833	17.41

Fig.S5: Protein band intensity quantification. A Coomassie-stained SDS-PAGE gel with pooled fractions of a size exclusion chromatography with ETR1 nanodiscs. The blue frame indicates the area for the density measurement. Fiji (2.9.0) software was used for measurement and calculation. **B** Graph of the color intensity inside the blue frame. Peaks marked by black arrows correspond to the protein bands of ETR1 and MSP1E3. The integrated areas of the peaks are shown in the table below in pixel² as well as in density values.

Experimental Section

Heterologous Expression

For heterologous expression, *E.coli* C43 (DE3) cells were transformed with 50 ng pETEV16b-AtETR1 and grown on 2YT-Agar plates (+Amp^{100}) at 37°C overnight. 100mL of 2YT (+Amp^{100}) media was inoculated with a single colony and incubated overnight at 37°C shaking at 180 rpm. The main culture was started by adding 1/100 volumes of overnight culture to the vessel of a Labfors 4 (INFORS HT) containing standard M9 minimal media (+Amp^{50}). For NMR analyses M9 media was supplemented with 15N-labeled NH_4Cl prior inoculation. The culture was incubated at 30°C with setpoints for pH= 6.80, pO2= 55 %, and a variable cascade setting of stirrer (250-1050 rpm) > airflow (2-5 L / min) until reaching OD 0.8. The temperature was then reduced to 16°C and the protein expression was induced by adding 0.5 mM IPTG. Cells were harvested 18 h after induction by centrifugation (7500xg, 15min, 4°C), frozen in liquid N_2 and stored at -20°C.

Isolation, Solubilisation and purification of ETR1

The isolation, solubilization and purification of ETR1 were carried out as previously described.[1] Depart from the referred procedure, 1.5 % (w/v) of n-Tetradecyl-phosphocholine (Fos-Choline-14, Glycon Biochemicals, Fürstenwalde, Germany) was used for the initial solubilization and 0.03 % (w/v) for all adjacent purification steps. During the sequential preparation, samples were taken and characterized by SDS-PAGE and Western-Blot. The purity of ETR1 was found to be greater than 95 %.

Expression and purification of MSP

The general expression and purification of MSP1E3 was executed as previously described.[2]

Protein Labeling

MSP1E3 was labeled with Alexa Fluor™ 555 NHS-Ester Dye, while ETR1 was labelled with Alexa Fluor™ 488 NHS-Ester Dye (Thermo Fischer Scientific, Waltham, United States). The labeling was carried out according to the manufacturer guidelines and the Molecular Probes® Handbook. The labeling efficiency was determined via spectroscopy and presented a molar ratio of 0.75 for ETR1 and 1.66 for MSP1E3.

Reconstitution of ETR1 in phospholipid nanodiscs

For the reconstitution of ETR1 in phospholipid nanodiscs, purified MSP1E3 scaffold protein and 1,2-dimyristoyl-sn-glycero-3-phosphocholine (DMPC; Avanti Polar Lipids, Inc., Alabaster, United States) were used. The reconstitution mixture for ETR1 loaded nanodiscs contained molar ratios of 2:2:240 ETR1, MSP1E3 and DMPC respectively. First, the samples were incubated at 25°C with 50mM Tris pH8.0, 200mM NaCl, 0.3% (w/v) foscholine-14 in an overhead shaker for 1h. Then washed and water-equilibrated Bio-Beads (Bio-Rad Laboratories, Inc., Hercules, United States) (0.8g per mL sample volume) were sequentially added over a period of 18 hours. The supernatant containing the loaded discs was then decantated and aggregates were removed by centrifugation (30.000 xg, 30min). The sample (500 µL) was then loaded on a 10/300 Superose-6 column and eluted in 0.2 mL fractions. Pooled fractions containing the majority of loaded discs were concentrated using an ultra-centrifugal filter (MWCO: 100kDa) and stored at 4°C. As a negative control, empty nanodiscs were prepared identically to the protocol for loaded discs apart from the stoichiometry of MSP1E3 and DMPC lipids which was adjusted to 2:300 respectively.

Size exclusion chromatography and detection of Fluorescence labeled nanodiscs

The reconstitution of Alexa-488™ labeled ETR1 in nanodiscs using Alexa-555™ labeled MSP was performed using the same protocol as for unlabeled nanodiscs. The sample containing the labeled discs was loaded onto a Superose™ 6 Increase 10/300 GL column which was equilibrated with SEC buffer (Tris pH8.0, 200 mM NaCl) and eluted with constant flow of 0.3 mL/min in fractions of 0.2 mL. The absorbance was simultaneously detected at wavelengths of 280 nm, 488 nm and 555 nm using the ÄKTA Explorer FPLC system (GE Healthcare). Samples of the eluted fractions that corresponded to the prominent peaks were taken and analyzed by SDS-PAGE. Fluorescence was detected using an Amersham™ Imager 680 device.

To estimate the size and molecular weight of the reconstituted nanodiscs, the Superose™ 6 Increase 10/300 GL column was calibrated with proteins of defined sizes between 660.000 and 6.500 Da (Thyroglobulin, Ferritin, Conalbumin, Ovalbumin, Ribonuclease A, Aprotinin) taken from gel filtration calibration kits for high molecular weight (HMW) #28403842 and low molecular weight (LMW) #28403841 (Cytivia, Marlborough, US). The calibration standards were individually diluted according to the gel filtration calibration kit manual. 500 µL of each individual sample was loaded on the column, which was equilibrated with SEC buffer (Tris pH8.0, 200 mM NaCl) and eluted with a constant flow of 0.3 mL/min. The elution volume of each standard was plotted against the decadic logarithm of the molecular weight (Fig. S4). A linear fit was applied to the plot to estimate the molecular weight of the reconstituted nanodiscs.

Protein band intensity quantification

An image of a coomassie-stained SDS-PAGE gel with pooled fractions of a size exclusion chromatography with ETR1 nanodiscs was opened by Fiji (ver.2.9.0) and converted to 8-bit grayscale format. The lane containing the bands of interest was enframed and selected for intensity measurement using the Analyze->Gel->Select first lane command (Fig. 5A). The Analyze->Gel->Plot lanes command was used to plot the color intensities inside the selected frame. The base of the peaks corresponding to ETR1 and MSP1E3 were drawn manually by using the freehand line tool in order to subtract the background noise. The areas of the enframed peaks were calculated using the wand (tracing) tool while the density percentages were calculated using the Analyze->Gel->Label Peaks command (Fig. 5B). The ratio of the band intensities was calculated by dividing the density percent of the ETR1 band (11.94) by the density percent of the MSP1E3 band (17.41) and resemble ≈0.69.

Nucleotide Binding Assay

10 µM of ETR1-NDs were co-incubated with 1 mM 2'/3'-O-(N-Methyl-anthraniloyl)-adenosine-5'-triphosphate (MANT-ATP, Jena Bioscience GmbH, Jena, Germany) 10min at room temperature followed by 30min incubation on ice in 50 mM Tris pH 8.0, 200 mM NaCl, 50 mM KCl, 20 mM MgCl2. Unbound MANT-ATP was removed by gel-filtration with a Zeba Spin-desalting column (Thermo Fisher Scientific, Waltham, US). Unlabeled ATP was added to the flow-through in a 10-fold excess (10 mM) to compete off MANT-ATP. Fluorescence emission spectra were detected from 380nm to 600nm wavelength with an LS55 fluorescence spectrometer (Perkin-Elmer, Waltham, United States) using a 45µL cuvette, 355 nm excitation, 5,0 nm slit width. Negative controls included samples of ETR1-ND co-incubated with MANT-ATP in the absence of Mg^{2+}, empty nanodiscs and a water control with MANT-ATP.

Small-angle X-ray scattering

We collected the SEC-SAXS data of empty nanodisc and ETR1 reconstituted in nanodisc on beamline BM29 at the ESRF Grenoble. [3] The sample to detector distance of the BM29 beamline was 2.827 m results in an achievable q-range of 0.03 – 5.2 nm^{-1}. The measurements were performed at 10°C with a protein concentration of 17.00 mg/ml for the empty Nanodisc and 5.6 mg/ml for ERT1 reconstituted in nanodisc. The SEC-SAXS run was performed on a Superose6 increase 10/300 GL column (100 µl inject, Buffer: 50mM Tris pH 8.0, 200 mM NaCl) with a flow rate of 0.5 ml/min. We collected 800 frames for each protein sample with an exposer time of 4 sec/frame. Data were scaled to absolute intensity against water.

All used programs for data processing were part of the ATSAS Software package (Version 3.0.5)[4]. Primary data reduction was performed with the programs CHROMIXS [5] and PRIMUS [6]. With the Guinier approximation [7], we determine the forward scattering *I(0)* and the radius of gyration (R_g). The program GNOM [8] was used to estimate the maximum particle dimension (D_{max}) with the pair-distribution function *p(r)*.

NMR spectroscopy

Two-dimensional 1H-15N NMR correlation spectra (HMQC-type) were recorded on 120 µM 15N ETR1 embedded in DMPC nanodiscs and dissolved in 20 mM sodium phosphate pH 6.5 buffer containing 200 mM NaCl. NMR experiments were performed on a Bruker 900 MHz AVANCE neo spectrometer equipped with a triple-resonance 1H,15N,13C cryogenic probe. The experimental temperature was 10°C. Spectral dimensions were 16.34 ppm (1H) x 35 ppm (15N), with 1024 complex points recorded in the 1H dimension and 64 complex points recorded in the 15N dimension, and the States-TPPI scheme used for quadrature detection, resulting in an acquisition time of 69 ms in the 1H dimension and 20 ms in the 15N dimension. The carrier was positioned at 4.7 ppm in the 1H dimension and 117 ppm in the 15N dimension; 2048 scans were recorded for each increment, with a recovery delay of 2 s between scans, resulting in an overall experimental time of 6.5 d.

NMR spectra were processed using the Bruker TopSpin 4.1.3 software. Spectra were zero-filled up to 2048 x 1024 complex points. A cosine squared window function and forward linear prediction was applied, including polynomial baseline correction. Spectra were plotted using the CCPN AnalysisAsign 3.0.4 software.

References

[1] S. Schott-Verdugo, L. Muller, E. Classen, H. Gohlke, G. Groth, *Sci Rep* **2019**, *9*, 8869.

[2] T. H. Bayburt, Y. V. Grinkova, S. G. Sligar, *Nano Letters* **2002**, *2*, 853-856.

[3] aP. Pernot, P. Theveneau, T. Giraud, R. N. Fernandes, D. Nurizzo, D. Spruce, J. Surr, S. McSweeney, A. Round, F. Felisaz, L. Foedinger, A. Gobbo, J. Huet, C. Villard, F. Cipriani, *Journal of Physics: Conference Series* **2010**, *247*, 012009; bP. Pernot, A. Round, R. Barrett, A. De Maria Antolinos, A. Gobbo, E. Gordon, J. Huet, J. Kieffer, M. Lentini, M. Mattenet, C. Morawe, C. Mueller-Dieckmann, S. Ohlsson, W. Schmid, J. Surr, P. Theveneau, L. Zerrad, S. McSweeney, *Journal of synchrotron radiation* **2013**, *20*, 660-664.

[4] K. Manalastas-Cantos, P. V. Konarev, N. R. Hajizadeh, A. G. Kikhney, M. V. Petoukhov, D. S. Molodenskiy, A. Panjkovich, H. D. T. Mertens, A. Gruzinov, C. Borges, C. M. Jeffries, D. I. Svergun, D. Franke, *Journal of Applied Crystallography* **2021**, *54*.

[5] A. Panjkovich, D. I. Svergun, *Bioinformatics* **2017**.

[6] P. V. Konarev, V. V. Volkov, A. V. Sokolova, M. H. J. Koch, D. I. Svergun, *Journal of Applied Crystallography* **2003**, *36*, 1277-1282.

[7] A. Guinier, *Annales de Physique* **1939**, *11*, 161-237.
[8] D. I. Svergun, *Journal of Applied Crystallography* **1992**, *25*, 495-503.